Optical pulse compression in dispersion decreasing photonic crystal fiber

J. C. Travers[1*]**, J. M. Stone**[2]**, A. B. Rulkov**[1]**, B. A. Cumberland**[1]**,**
A. K. George[2]**, S. V. Popov**[1]**, J. C. Knight**[2]** and J. R. Taylor**[1]

[1]*Femtosecond Optics Group, Department of Physics, Prince Consort Road,*
Imperial College London, London SW7 2AZ, UK
[2]*Centre for Photonics and Photonic Materials, Department of Physics, University of Bath,*
Claverton Down, Bath BA2 7AY, UK
*Corresponding author: john.travers@imperial.ac.uk

Abstract: Improvements to tapered photonic crystal fiber (PCF) fabrication have allowed us to make up to 50 m long PCF tapers with loss as low as 30 dB/km. We discuss the design constraints for tapered PCFs used for adiabatic soliton compression and demonstrate over 15 times compression of pulses from over 830 fs to 55 fs duration at a wavelength of 1.06 μm, an order of magnitude improvement over previous results.

References and links

1. S. V. Chernikov and P. V. Mamyshev, "Femtosecond Soliton Propagation in Fibers with Slowly Decreasing Dispersion," J. Opt. Soc. Am. B **8**, 1633–1641 (1991).
2. K. Smith and L. F. Mollenauer, "Experimental-Observation of Adiabatic-Compression and Expansion of Soliton Pulses over Long Fiber Paths," Opt. Lett. **14**, 751–753 (1989).
3. J. C. Knight, T. A. Birks, P. S. Russell, and D. M. Atkin, "All-silica single-mode optical fiber with photonic crystal cladding," Opt. Lett. **21**, 1547–1549 (1996).
4. V. Gapontsev, D. Gapontsev, N. Platonov, O. Shkurikhin, V. Fomin, A. Mashkin, M. Abramov, and S. Ferin, "2 kW CW ytterbium fiber laser with record diffraction-limited brightness," in *Conference on Lasers and Elctro-Optics Europe*, p. 508 (IEEE, Munich, Germany, 2005).
5. R. E. Kennedy, A. B. Rulkov, S. V. Popov, and J. R. Taylor, "High-peak-power femtosecond pulse compression with polarization-maintaining ytterbium-doped fiber amplification," Opt. Lett. **32**, 1199–201 (2007).
6. J. Limpert, F. Roser, T. Schreiber, and A. Tunnermann, "High-power ultrafast fiber laser systems," IEEE J. Sel. Top. Quantum Electron. **12**, 233–244 (2006).
7. A. B. Rulkov, M. Y. Vyatkin, S. V. Popov, J. R. Taylor, and V. P. Gapontsev, "High brightness picosecond all-fiber generation in 525-1800nm range with picosecond Yb pumping," Opt. Express **13**, 377–381 (2005).
8. C. V. Shank, R. L. Fork, R. Yen, R. H. Stolen, and W. J. Tomlinson, "Compression of Femtosecond Optical Pulses," Appl. Phys. Lett. **40**, 761–763 (1982).
9. L. F. Mollenauer, R. H. Stolen, J. P. Gordon, and W. J. Tomlinson, "Extreme Picosecond Pulse Narrowing by Means of Soliton Effect in Single-Mode Optical Fibers," Opt. Lett. **8**, 289–291 (1983).
10. S. V. Chernikov, E. M. Dianov, D. J. Richardson, and D. N. Payne, "Soliton Pulse-Compression in Dispersion-Decreasing Fiber," Opt. Lett. **18**, 476–478 (1993).
11. S. V. Chernikov, D. J. Richardson, E. M. Dianov, and D. N. Payne, "Picosecond Soliton Pulse Compressor Based on Dispersion Decreasing Fiber," Electron. Lett. **28**, 1842–1844 (1992).
12. R. E. Kennedy, S. V. Popov, and J. R. Taylor, "Compact fully fibre integrated source of 100 fs pulses at 1.1 mu m based on compression in holey fibre," Electron. Lett. **41**, 234–235 (2005).
13. A. Mostofi, H. Hatami-Hanza, and P. L. Chu, "Optimum dispersion profile for compression of fundamental solitons in dispersion decreasing fibers," IEEE J. Quantum Electron. **33**, 620–628 (1997).
14. K. Tajima, "Compensation of Soliton Broadening in Nonlinear Optical Fibers with Loss," Opt. Lett. **12**, 54–56 (1987).

15. A. S. Gouveianeto, P. G. J. Wigley, and J. R. Taylor, "Soliton Generation through Raman Amplification of Noise Bursts," Opt. Lett. **14**, 1122–1124 (1989).
16. P. C. Reeves-Hall, S. A. E. Lewis, S. V. Chenikov, and J. R. Taylor, "Picosecond soliton pulse-duration-selectable source based on adiabatic compression in Raman amplifier," Electron. Lett. **36**, 622–624 (2000).
17. M. D. Pelusi and H. F. Liu, "Higher order soliton pulse compression in dispersion-decreasing optical fibers," IEEE J. Quantum Electron. **33**, 1430–1439 (1997).
18. G. Humbert, W. J. Wadsworth, S. G. Leon-Saval, J. C. Knight, T. A. Birks, P. S. J. Russell, M. J. Lederer, D. Kopf, K. Wiesauer, E. I. Breuer, and D. Stifter, "Supercontinuum generation system for optical coherence tomography based on tapered photonic crystal fibre," Opt. Express **14**, 1596–1603 (2006).
19. A. Kudlinski, A. K. George, J. C. Knight, J. C. Travers, A. B. Rulkov, S. V. Popov, and J. R. Taylor, "Zero-dispersion wavelength decreasing photonic crystal fibers for ultraviolet-extended supercontinuum generation," Opt. Express **14**, 5715–5722 (2006).
20. J. C. Travers, A. B. Rulkov, S. V. Popov, J. R. Taylor, A. Kudlinski, A. K. George, and J. C. Knight, "Dispersion-Decreasing PCF for Blue-UV Supercontinuum Generation," in *Conference on Lasers and Elctro-Optics*, p. CPDA11 (Optical Society of America, Long Beach, CA, USA, 2006).
21. M. L. V. Tse, P. Horak, J. H. V. Price, F. Poletti, F. He, and D. J. Richardson, "Pulse compression at 1.06 mu m in dispersion-decreasing holey fibers," Opt. Lett. **31**, 3504–3506 (2006).
22. J. C. Knight, J. Arriaga, T. A. Birks, A. Ortigosa-Blanch, W. J. Wadsworth, and P. S. J. Russell, "Anomalous dispersion in photonic crystal fiber," IEEE Phot. Tech. Lett. **12**, 807–809 (2000).
23. M. Midrio, M. P. Singh, and C. G. Someda, "The space filling mode of holey fibers: An analytical vectorial solution," J. Lightwave Technol. **18**, 1031–1037 (2000).
24. K. J. Blow and D. Wood, "Theoretical Description of Transient Stimulated Raman-Scattering in Optical Fibers," IEEE J. Quantum Electron. **25**, 2665–2673 (1989).
25. P. L. Francois, "Nonlinear Propagation of Ultrashort Pulses in Optical Fibers - Total Field Formulation in the Frequency-Domain," J. Opt. Soc. Am. B **8**, 276–293 (1991).
26. O. V. Sinkin, R. Holzlohner, J. Zweck, and C. R. Menyuk, "Optimization of the split-step Fourier method in modeling optical-fiber communications systems," J. Lightwave Technol. **21**, 61–68 (2003).
27. D. Hollenbeck and C. Cantrell, "Multiple-vibrational-mode model for fiber-optic Raman gain spectrum and response function," J. Opt. Soc. Am. B **19**, 2886–2892 (2002).
28. R. H. Stolen, J. P. Gordon, W. J. Tomlinson, and H. A. Haus, "Raman Response Function of Silica-Core Fibers," J. Opt. Soc. Am. B **6**, 1159–1166 (1989).
29. E. M. Dianov, Z. S. Nikonova, A. M. Prokhorov, and V. N. Serkin, "Optimal compression of multi-soliton pulses in optical fibers," Sov. Tech. Phys. Lett. **12**, 311–313 (1986).
30. P. V. Mamyshev, P. G. J. Wigley, J. Wilson, G. I. Stegeman, V. A. Semenov, E. M. Dianov, and S. I. Miroshnichenko, "Adiabatic compression of Schrödinger solitons due to the combined perturbations of higher-order dispersion and delayed nonlinear response," Phys. Rev. Lett. **71**, 73–76 (1993).

1. Introduction

Pulse compression in optical fiber can be used to provide controllable sources of ultrashort pulses for many applications. One of the most compact and versatile compression schemes is adiabatic soliton compression (ASC) in long lengths of dispersion decreasing fiber, which guarantees bandwidth limited output while still offering very high compression ratios [1, 2]. Until recently, ASC had not been demonstrated at wavelengths shorter than $\sim 1.3\ \mu$m because it requires anomalous group velocity dispersion, which is unachievable in conventional single-mode optical fiber below this wavelength. With the recent introduction of photonic crystal fiber (PCF) anomalous dispersion at shorter wavelengths has become possible [3], and by tapering PCF we can achieve an anomalous dispersion-decreasing fiber below 1.3 μm. Here we demonstrate use of a tapered PCF for 15-times pulse compression to sub 50 fs pulses at a wavelength of 1.06 μm using ASC, confirming that high pulse compression ratios can be obtained with tapered PCF. With suitable fiber design engineering, compression to the few-optical-cycle regime will be possible.

The 1.06 μm spectral region is a very important gain window for optical fiber lasers and amplifiers. The highest power CW and pulsed fiber-lasers have been demonstrated in this region [4–7]. A high quality pulse compression scheme in this spectral range is thus very desirable. The most successful fiber based pulse compression schemes demonstrated to date include fiber-grating compressors [8] and soliton effect compressors [9], along with adiabatic soliton

compressors which are the subject of this paper [1,2,10,11]. The first two techniques have been demonstrated and used many times at 1.06 μm [5,12].

2. Adiabatic soliton compression

Adiabatic soliton compression can be understood by considering the equation relating the soliton duration $\tau_0 = 0.568\tau_{FWHM}$ to the group-velocity dispersion coefficient β_2

$$\tau_0 = \frac{2N^2|\beta_2|}{\gamma E_s} \tag{1}$$

where $E_s = 2P_0\tau_0$ is the soliton energy, P_0 the peak power, N is the soliton order and $\gamma = 2\pi n_2/(cA_{eff})$ is the fiber nonlinearity coefficient, with A_{eff} the effective mode area of the fiber and n_2 the nonlinear refractive index. In what follows we also refer to the dispersion parameter $D = -2\pi c|\beta_2|/\lambda^2$ and the soliton length $z_s = \pi\tau_0^2/(2|\beta_2|)$ where c is the speed of light and λ is the wavelength.

Soliton propagation is adiabatic when the fiber parameters such as dispersion and nonlinearity, or the soliton energy (through gain or loss) vary slowly relative to the soliton length z_s [10]. In this regime the total energy is contained in the soliton, which behaves according to Eq. (1). In this case, it is clear that the soliton duration will change if either the dispersion or the nonlinearity is changed along the fiber. These parameters are changed by varying the core size (tapering) in a conventional fiber or by changing the microstructure parameters in a PCF. It has been shown that the length of the taper and the taper profile are not critical parameters for the soliton compression as long as the adiabatic condition is maintained by using sufficiently long tapers [13]. In this case, and neglecting the variation in γ, the input to output pulse duration ratio τ_0/τ_z is equal to the ratio of the input and output dispersion $\beta_2(0)/\beta_2(z)$. In practice, the soliton energy is not constant, due to the attenuation of the fiber. This reduction of soliton energy leads to pulse broadening and so must be compensated for by additional dispersion decrease (indeed, this was the original inspiration for this technique [14]). In contrast, additional gain increases the soliton energy and pulse compression can be achieved by this mechanism alone, typically using Raman amplifiers which are very well suited to provide the distributed gain required for adiabatic soliton propagation [15, 16]. Although true adiabatic compression is achieved by injecting $N = 1$ solitons it is possible to mitigate the effects of fiber loss and enhance the pulse compression by injecting pulses corresponding to $1 \leq N \leq 2$. This can lead to considerably higher compression ratios without significantly decreasing the pulse quality [17].

Outside of the adiabatic regime, the soliton will shed energy into non-solitonic radiation leading to spectral and temporal distortion of the pulse and therefore the useful pulse compression achievable will be limited. As the soliton length is proportional to the square of the pulse duration, this dictates that longer tapers are required for compression of longer pulses and hence for high compression ratios.

3. Design of dispersion decreasing PCF tapers

PCFs can provide very high anomalous waveguide dispersion and thus cancel the normal material dispersion of silica to produce optical fibers with anomalous dispersion at wavelengths as short as the visible. The decreasing dispersion required for ASC was achieved by using tapered PCF. Very short tapered photonic crystal fibers have previously been produced using simultaneous stretching and heating to post-process a fiber [18]. Last year, we demonstrated much longer photonic crystal fiber tapers which were produced at the drawing tower as the fiber was being drawn [19,20]. These were designed for blue and ultra-violet supercontinuum generation from a 1.06 μm pump source. Recently a small compression (factor of 2) was demonstrated in

a tapered PCF at 1.06 μm in an 8 m fiber [21]. The 2-fold decrease in dispersion and relatively high (150 dB/km) loss restricted the compression ratio. However, it is impossible to use these short tapers to achieve high compression ratios or to compress pulses longer than a few hundred femtoseconds because they are insufficiently long compared to the soliton period. In this paper we report tapers which are up to 50 m long and which have much lower loss, significantly broadening the range of applications for which tapered PCFs can be used. We report over 15 times pulse compression of pulses from over 800 fs to below 55 fs duration.

Many parameters are available for control in a PCF tapering process. A solid core PCF is defined by its pitch Λ (the distance between cladding air-holes) and cladding air-hole diameter d/Λ (Fig. 2 shows the structure of the PCFs used in this paper, where the pitch and air-hole diameter can be clearly observed). Adjustment of these parameters allows for great control of the dispersion and nonlinearity along the fiber [3, 22]. The fibers used in our experiments were produced after extensive numerical modelling with the generalized nonlinear Schrödinger equation to optimize the interplay between the loss, dispersion and nonlinearity. In particular, the change in γ can be very significant and care must be taken to ensure that it increases as D decreases or some cancelling of the compression effect will occur.

The dispersion profiles of the PCFs used in the simulations were calculated using a fully analytical vector effective-index method [23]. The propagation of the solitons through the optical fiber was calculated from the generalized nonlinear Schrödinger equation [24, 25], which we solved using an adaptive, symmetrized split-step Fourier method [26]. The simulations included the exact calculated dispersion and an accurate model of the measured Raman response of silica [27, 28].
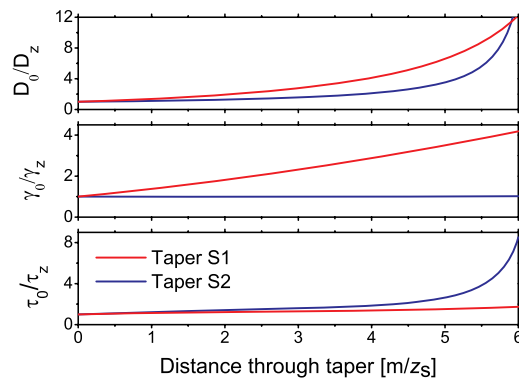

Fig. 1. Profiles of (a) the dispersion and (b) the nonlinearity along two illustrative tapers S1 (d/Λ constant at 0.8, Λ changing from 2 to 4.2 μm) and S2 (d/Λ changing from 0.55 to 0.44 and Λ changing from 1.76 to 1.56 μm). (c) The simulated pulse compression factors along the tapers. All are shown over a length corresponding to 6 soliton periods. The input pulse duration was $\tau_{FWHM} = 800$ fs and both tapers had a realistic loss of 25 dB/km.

To illustrate the importance of this interplay, Fig. 1 shows the results of numerical simulations of $N = 1$ soliton propagation in two tapered PCF structures which we investigated when designing our tapers. The first taper (S1) has a constant air-hole diameter to pitch ratio (d/Λ) while the pitch is increased by a factor of 2. This structure is similar to those we used for supercontinuum generation (though used here in reverse) [19, 20]. In this type of tapered PCF the zero dispersion wavelength moves to longer wavelengths (and towards the pump wavelength) and hence the dispersion at the fixed pump wavelength of 1.06 μm decreases. However, the nonlinearity γ also decreases as the effective area increases. The net result is much less compression than expected from the ratio of input to output dispersion values. In the specific case

of Taper S1 shown in Fig. 1, the dispersion ratio is 12 but compression is less than a factor of 2. In the second taper (S2) the air-hole diameter to pitch ratio is reduced by 20% and the pitch is reduced by just over 11%. This structure is similar to that used in the experiments described below. In this case, the dispersion at the pump wavelength decreases as the second zero dispersion wavelength of the fiber moves to shorter wavelengths. But in contrast to taper S1, the effective core stays approximately constant and hence so does the nonlinearity. In the specific case of Taper S2, the dispersion ratio is 13 but the simulated compression factor is over 8. By analyzing the PCF dispersion profiles in this way we determined that to achieve high compression ratios in PCF tapers it is advantageous to work around the second zero dispersion wavelength of the fiber, as this allows for decreasing the dispersion while maintaining the nonlinearity.

4. Fabrication of dispersion decreasing PCF tapers

(a) Taper A input   (b) Taper A output

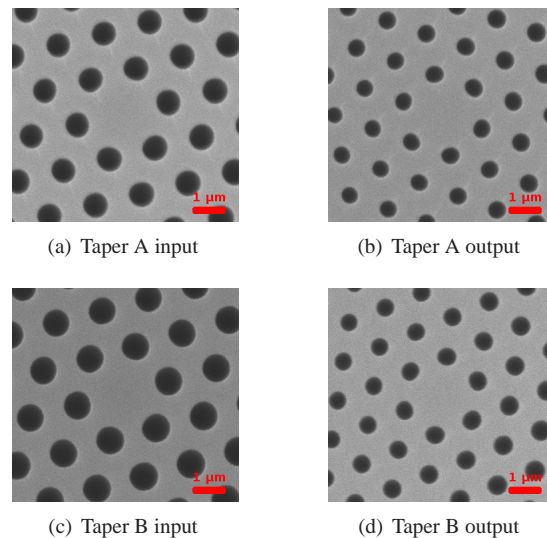(c) Taper B input   (d) Taper B output

Fig. 2. Scanning electron micrographs of the input and output ends of the tapers.

Our tapered PCFs were produced by the conventional stack and draw process [3]. However, during the final draw down to fiber, the pitch and air-hole diameter were varied by stopping the preform feed and then restarting it in a controlled manner while simultaneously adjusting the air-hole pressure. This resulted in two tapers we label A and B. Figure 2 shows SEM images of the tapers. From these we measured the hole diameter to pitch ratio of Taper A to vary from 0.52 to 0.42 and the pitch to change from 1.44 to 1.25 μm. For Taper B the hole diameter to pitch ratio varies from 0.55 to 0.45, and the pitch changes from 1.48 to 1.20 μm.

The dispersion of the fibers was measured using an interferometric technique. A short section ($\sim$ 40 mm) of fiber was placed in one arm of a Mach-Zehnder interferometer equipped with a moveable mirror. An optical supercontinuum was used as a light source, and spectral interferograms were recorded for different values of the delay. From this the group delay was obtained, and used to find the group velocity dispersion. Figure 3 shows the measured dispersion curves for the two tapers. Taper A was 17 m long and had a measured dispersion changing from D $\sim$ 33 to$\sim$ -5 ps nm^{-1} km^{-1} at 1.06 μm. Taper B was 56 m long and had a measured dispersion varying from D $\sim$ 40 to 10 ps nm^{-1} km^{-1}. In both tapers the attenuation was measured by the cut-back technique to be around 30 dB/km in the spectral range of interest.
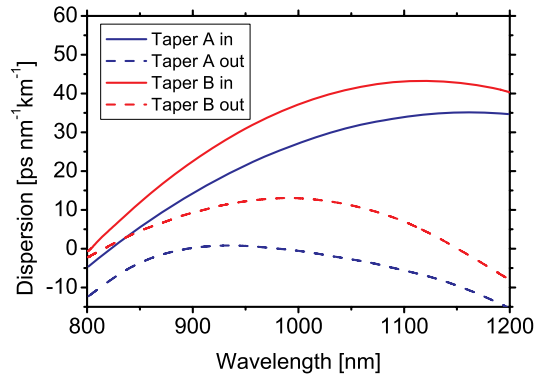
Fig. 3. The measured dispersion profiles of Taper A (blue) and Taper B (red).

The nonlinearity of both fibers varies from about 40 to 50 W^{-1} km^{-1} with the core diameter varying from 2.2 to 2 μm.

Although the dispersion of Taper A is slightly normal at the output, it is so only for a very short propagation length at the end of the taper (estimated from the previous cut-back of the taper), therefore we expect it to have only a small influence on the pulse compression process.
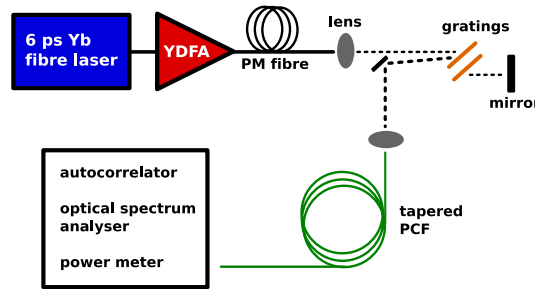
5. Experiment

Fig. 4. Experimental setup for pumping the dispersion decreasing PCF. YDFA = ytterbium doped fiber amplifier; PM = polarization maintaining.

The tapered PCFs were pumped with pulses from the fiber-grating compressor setup shown in Fig. 4. A SESAM based mode-locked fiber laser producing linearly polarized 6 ps pulses was used as a seed source. This was amplified by an ytterbium fiber amplifier (output power ~35 mW) and then passed through a length of normally dispersive polarization maintaining fiber (~20 m) to apply a selective degree of approximately linear chirp to the seed pulses. Complete compensation of the chirp was achieved by varying the separation of a pair of transmission gratings. Thus we could provide pulses of between 100 and 900 fs by varying the length of the chirping fiber, the input power and the grating separation. The pulses always had a time-bandwidth product of less than 0.75. These were then injected into the tapers with a coupling efficiency of approximately 60% and the output pulses were analyzed using a second-harmonic generation autocorrelator and an optical spectrum analyzer. The pulse energy was controlled using a half-wave plate before the polarized transmission gratings. The polarization of the pulses entering the tapered fiber was adjusted by an additional wave plate. The input pulse durations

were optimized for the highest compression ratio in each taper. For Taper A, 655 fs pulses were used; for Taper B, 830 fs pulses were used.
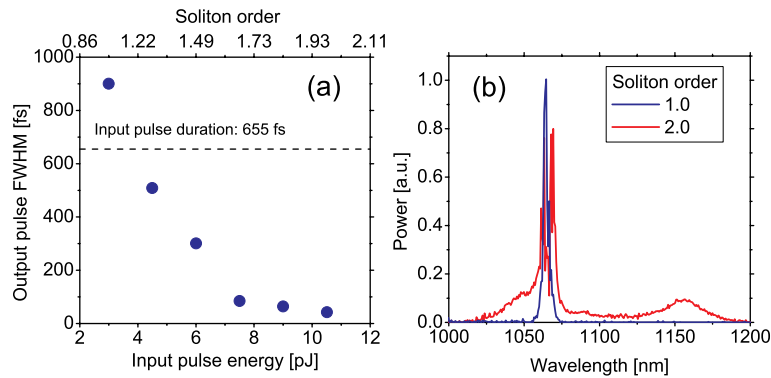

Fig. 5. (a) Output pulse duration (FWHM) from Taper A for given soliton energy (input $\tau_{FWHM} = 655$ fs); spectra of the output pulses at $N = 1$ and $N = 2$.
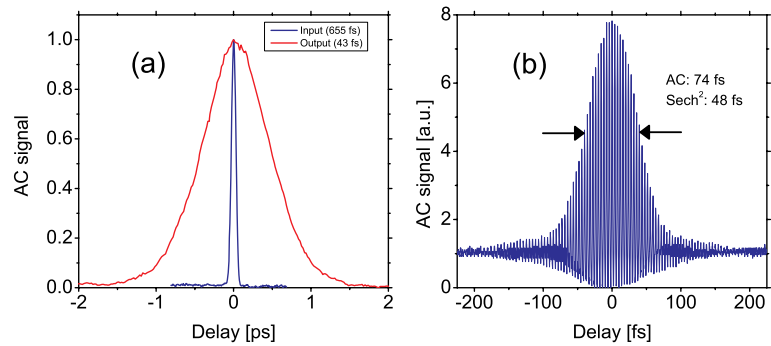

Fig. 6. (a) Autocorrelations of the input to Taper A and output for $N = 2$.; (b) fringe-resolved autocorrelation of the output pulse at $N = 2$.

The results for Taper A are shown in Fig. 5 and Fig. 6. The highest order soliton of $N = 2$ compressed to a pulse of sub 50 fs duration, a compression factor of over 13. It should be noted that the optimal soliton effect compression (SEC) of an N=2 soliton in an optimal fiber length will be a factor of 8 [29], this would occur in a fibre length of 4.7 m and subsequent propagation would degrade the compression. Here we have a suboptimal SEC length and so the decreasing dispersion is clearly significant for obtaining the 13 times compression observed. However, the soliton length $z_s = 11$ m in this taper, and thus the taper length of 17 m is insufficient for adiabatic compression alone. It is the combined effect of SEC and decreasing dispersion which achieves the pulse compression ratio of 13 in this taper as discussed in [17]. We believe that the output pulse duration from Taper A was inhibited slightly by the onset of normal dispersion at the end of the taper. Evidence of this can be seen from the spectra shown in Fig. 5(b) where for the $N = 2$ input, a dispersive wave at long wavelengths is observed. The compressed soliton is

actually shifted to shorter wavelengths around 1050 nm and could be filtered from the dispersive components if desired.

The short taper length with respect to z_s and the normal dispersion at the end of the taper are the reason that a higher compression ratio for an $N = 1$ soliton was not achieved.
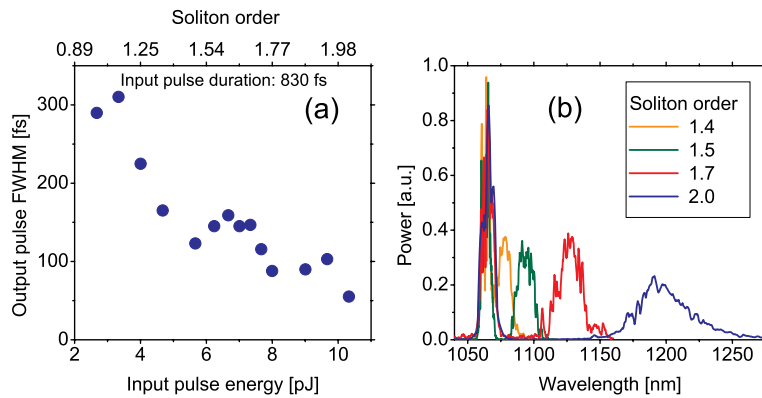

Fig. 7. (a) Output pulse duration (FWHM) from Taper B for given soliton energy (input $\tau_{FWHM} = 830$ fs); (b) spectra of the output pulses at various soliton orders.
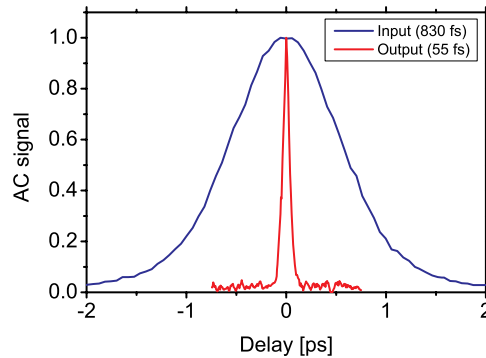

Fig. 8. Autocorrelations of the input to Taper B and output for $N = 2$.

The results for Taper B are shown in Fig. 7 and Fig. 8. Compression to a 55 fs pulse was achieved at the highest pulse input soliton order $N = 2$, this is a compression factor of 15. In contrast to Taper A, a $N = 1$ soliton is compressed by a factor of 3 in this taper and hence the assistance of SEC is not required. However, a significant increase in compression is obtained for $N > 1$. The pulse spectra shown for the output of Taper B in Fig. 7(b) indicate soliton self-frequency shifting of the output solitons to longer wavelengths. By considering Fig. 3 it is clear that such a shift further decreases the dispersion and hence enhance the compression (although the dispersion at the very end of the taper is normal at 1200 nm it will be only for the very end of the taper and hence will not have significantly broadened the output pulses). This explains why the compression factor is so much higher than that expected from the dispersion ratio at the pump wavelength alone. We should note here that the use of the Raman shift to cause a soliton

to compress through decreasing dispersion in a non-tapered fiber has also been observed [30]. From the spectra in Fig. 7(b) we confirmed that the time bandwidth product of the solitons was 0.31.

6. Conclusion

In conclusion, we have demonstrated pulse compression ratios of over 15 in dispersion decreasing PCF by utilizing soliton compression at $1.06\ \mu$m. Pulses as short as than 55 fs have been produced from input pulses of 830 fs. This demonstration has proved that the use of PCF tapers can enable high pulse compression ratios through adiabatic soliton compression at wavelengths where it is impossible to use conventional optical fiber. By further reducing the fiber loss and by careful control of the third order dispersion it should be possible to produce even shorter pulses. This technique can also be used in many other regimes. By moving to the $1.55\ \mu$m wavelength region and correctly engineering the PCF taper, simulations indicate that few-cycle pulses may be achievable. Alternatively, the use of PCF tapers may allow for compression of pulses at visible wavelengths.